

Constraints on Supersymmetric Flavor Changing Parameters

Using $B \rightarrow PP$ Decays

Dilip Kumar Ghosh, Xiao-Gang He, Yu-Kuo Hsiao and Jian-Qing Shi

Department of Physics, National Taiwan University, Taipei, Taiwan 10764, R.O.C.

Abstract

We study contributions of quark-squark-gluino interactions in Minimal Supersymmetric Standard Model (MSSM) to $B \rightarrow PP$ ($PP = K\pi, \pi\pi, KK$) decays using QCD improved factorization method for the evaluation of the hadronic matrix elements and taking into account renormalization group running of the Wilson coefficients from SUSY scale ($\approx m_{\tilde{q}}$) to the low energy scale ($= m_b$) applicable to B decays. Using the most recent experimental data we obtain constraints on flavor changing Supersymmetric (SUSY) parameters $(\delta_{ij})_{LL,RR}$. For $\Delta S = -1$ processes, $b \rightarrow s\gamma$ is usually considered to give the strongest limits. We, however, find that in some part of the parameter space $B \rightarrow K\pi$ processes give stronger bounds. Implications for $B_s^0 - \bar{B}_s^0$ mixing is discussed. We also study constraints obtained from $\Delta S = 0$ processes $B \rightarrow \pi\pi, KK, \rho\gamma$ and $B_d - \bar{B}_d$ mixing. In this case, in a large part of the parameter space $B_d - \bar{B}_d$ provides the best bound, but $B \rightarrow K^- K^0, \rho\gamma$ can still give interesting constraints in a complementary region of the parameter space.

I. INTRODUCTION

Recent results from B -factories at CLEO, BaBar, Belle have attracted a lot of attentions. Data from these experiments provide new opportunities to further study the Standard Model (SM) and also to study physics beyond the SM. Rare charmless hadronic B decays, such as $B \rightarrow PP (PP = K\pi, \pi\pi, KK)$, are particularly interesting. These processes being rare are sensitive to new physics beyond the SM. Minimal Supersymmetric Standard Model (MSSM), which is an extension of the SM emerges as one of the most promising candidates for new physics beyond the SM. MSSM resolve many of the potential problem of the SM, for example the hierarchy problem, unification of $SU(3) \times SU(2) \times U(1)$ gauge couplings, and so on [1].

$B \rightarrow PP$ decays have been studied extensively within the framework of naive factorization scheme. In the last few years, QCD improved factorization method have been developed. This method incorporates elements of the naive factorization approach (as its leading term) and perturbative QCD corrections (as subleading contributions) allowing one to compute systematic radiative corrections to the naive factorization for the hadronic B decays [2,3]. This method provides a better understanding of the strong interaction dynamics for B decay into two light mesons. Therefore results obtained using QCD improved method are expected to be more reliable compared with those obtained by using naive factorization. Lot of studies have been done in this direction so far [4,5].

In this paper we study implications of the recently measured $B \rightarrow PP$ branching ratios on SUSY flavor changing parameters, specially arising from the quark-squark-gluino ($q - \tilde{q} - \tilde{g}$) interactions in the model [6]. Effects of SUSY interactions on various processes involving B mesons have been studied previously [6–11]. Here we will concentrate on the $q - \tilde{q} - \tilde{g}$ interactions and re-analyze $B \rightarrow PP$ decays with several improvements. Firstly we use the QCD improved factorization method to compute the two body hadronic B decays. Secondly, we improve the quark level effective Hamiltonian by including QCD running of different Wilson coefficients (WC) from the SUSY scale ($= m_{\tilde{q}}$) to the low energy scale ($= m_b$) which is applicable to B decays. Previous authors while doing similar analysis have neglected this

RG evolution of WC's. We find that this RG evolution of WC's have non-negligible effects on the branching ratio calculations.

Using the most recent experimental data from different B -factories on the $B \rightarrow PP$ decays we constrain the flavor changing SUSY parameters arising from the $\tilde{q}_{iLR} - \tilde{q}_{jLR}$ mixing due to the presence of $q - \tilde{q} - \tilde{g}$ interaction vertices in different one loop contributions to $B \rightarrow PP$ decays. Similar kind of squark mixing can also occur for other flavor changing B decays. For $\Delta S = -1$ processes, $b \rightarrow s\gamma$ is usually considered to give the strongest limit on such mixing. We, however, find that in some part of the parameter space $B \rightarrow K\pi$ processes provide better bound. We also discuss the implications of $B_s^0 - \bar{B}_s^0$ mixing in this context. Furthermore, we also study constraints on FCNC parameters obtained from $\Delta S = 0$ processes $B \rightarrow \pi\pi, KK, \rho\gamma$, and $B_b - \bar{B}_d$ mixing. We find that $B_d^0 - \bar{B}_d^0$ mixing provides the best limit in a large part of the parameter space, but in certain region of the parameter space $B \rightarrow \pi\pi, KK, \rho\gamma$ can still give better constraints.

II. SQUARK-GLUINO CONTRIBUTIONS TO $B \rightarrow PP$ DECAYS

In the SUSY, squark and gluino induce large one loop contribution to $B \rightarrow PP$ decay from penguin and box diagrams because they are related to strong couplings. We compute the effect of flavor changing contributions to $B \rightarrow PP$ arising from $q - \tilde{q} - \tilde{g}$ interaction vertices using the mass insertion approximation method [6,12]. In this method, the basis of the quark and squark states are chosen in such a way that their couplings with gluinos are flavor diagonal. The flavor changing current arises from the non-diagonality of the squark propagators. We denote the off-diagonal terms in the squark mass matrices (i.e. the mass terms relating squark of the same electric charge, but different flavor), by Δ , then we expand the squark propagators as series in terms of $(\delta_{ij})_{AB} = (\Delta_{ij})_{AB}/\tilde{m}^2$ where \tilde{m} is an average squark mass, $A, B = L, R$ and i, j are the generation indices. The notation $(\delta_{13})_{AB}$ and $(\delta_{23})_{AB}$ denote $\tilde{d} - \tilde{b}$ and $\tilde{s} - \tilde{b}$ mixing respectively. These two parameters signify the size of flavor changing interactions in SUSY through the $q - \tilde{q} - \tilde{g}$ interactions.

At one loop level, for $\tilde{q}_L - \tilde{q}_L$ mixing (LL type), the new effective Hamiltonian relevant to $B \rightarrow K\pi, \pi\pi$ decays arise from SUSY penguin and box diagrams with gluino-squark in the loops is given by

$$H_{eff}^{susy} = -\frac{G_F}{\sqrt{2}} V_{tb} V_{tq}^* \sum_{i=3}^6 C_i^{LL} O_i. \quad (1)$$

Here we have normalized the WC's according to the SM ones. The operator O_i is the same as SM definition with

$$\begin{aligned} O_3 &= \bar{q}_i \gamma^\mu L b_i \sum_{q'} \bar{q}'_j \gamma_\mu L q'_j, \quad O_4 = \bar{q}_i \gamma^\mu L b_j \sum_{q'} \bar{q}'_j \gamma_\mu L q'_i, \\ O_5 &= \bar{q}_i \gamma^\mu L b_i \sum_{q'} \bar{q}'_j \gamma_\mu R q'_j, \quad O_6 = \bar{q}_i \gamma^\mu L b_j \sum_{q'} \bar{q}'_j \gamma_\mu R q'_i, \end{aligned} \quad (2)$$

where $L(R) = (1 \pm \gamma_5)$, $q = d, s$, $q' = u, d, s$. The WC's are given by [6]:

$$\begin{aligned} C_3^{LL}(M_{susy}) &= \frac{-\alpha_s^2}{2\sqrt{2}G_F V_{tb} V_{tq}^* m_{\tilde{q}}^2} (\delta_{j3})_{LL} \left(-\frac{1}{9} B_1(x) - \frac{5}{9} B_2(x) - \frac{1}{18} P_1(x) - \frac{1}{2} P_2(x) \right) \\ C_4^{LL}(M_{susy}) &= \frac{-\alpha_s^2}{2\sqrt{2}G_F V_{tb} V_{tq}^* m_{\tilde{q}}^2} (\delta_{j3})_{LL} \left(-\frac{7}{3} B_1(x) + \frac{1}{3} B_2(x) + \frac{1}{6} P_1(x) + \frac{3}{2} P_2(x) \right) \\ C_5^{LL}(M_{susy}) &= \frac{-\alpha_s^2}{2\sqrt{2}G_F V_{tb} V_{tq}^* m_{\tilde{q}}^2} (\delta_{j3})_{LL} \left(\frac{10}{9} B_1(x) + \frac{1}{18} B_2(x) - \frac{1}{18} P_1(x) - \frac{1}{2} P_2(x) \right) \\ C_6^{LL}(M_{susy}) &= \frac{-\alpha_s^2}{2\sqrt{2}G_F V_{tb} V_{tq}^* m_{\tilde{q}}^2} (\delta_{j3})_{LL} \left(-\frac{2}{3} B_1(x) + \frac{7}{6} B_2(x) + \frac{1}{6} P_1(x) + \frac{3}{2} P_2(x) \right) \end{aligned} \quad (3)$$

where $j = 1, 2$ when $q = d, s$, respectively and $x = m_g^2/m_{\tilde{q}}^2$. The definition of the functions $B_i(x), P_i(x)$ can be found in Ref [6].

The above WC's are obtained at the SUSY scale M_{susy} . We take this scale as $m_{\tilde{q}}$. We then evolve these WC's from this high scale down to the scale m_b using the RG equation. At the lower scale, after the RG evolution, the WC's take following form:

$$\begin{aligned} C_3^{LL}(m_b) &= b_3^3 C_3^{LL}(M_{susy}) + b_3^4 C_4^{LL}(M_{susy}) + b_3^5 C_5^{LL}(M_{susy}) + b_3^6 C_6^{LL}(M_{susy}) \\ C_4^{LL}(m_b) &= b_4^3 C_3^{LL}(M_{susy}) + b_4^4 C_4^{LL}(M_{susy}) + b_4^5 C_5^{LL}(M_{susy}) + b_4^6 C_6^{LL}(M_{susy}) \\ C_5^{LL}(m_b) &= b_5^3 C_3^{LL}(M_{susy}) + b_5^4 C_4^{LL}(M_{susy}) + b_5^5 C_5^{LL}(M_{susy}) + b_5^6 C_6^{LL}(M_{susy}) \\ C_6^{LL}(m_b) &= b_6^3 C_3^{LL}(M_{susy}) + b_6^4 C_4^{LL}(M_{susy}) + b_6^5 C_5^{LL}(M_{susy}) + b_6^6 C_6^{LL}(M_{susy}) \end{aligned} \quad (4)$$

M_{susy} (GeV)	b_3^3	b_3^4	b_3^5	b_3^6	b_4^3	b_4^4	b_4^5	b_4^6
100	1.144	-0.222	0.009	0.086	-0.322	0.989	-0.022	-0.197
500	1.208	-0.299	0.018	0.139	-0.432	1.002	-0.042	-0.298
1000	1.235	-0.328	0.022	0.164	-0.474	1.009	-0.051	-0.342
M_{susy} (GeV)	b_5^3	b_5^4	b_5^5	b_5^6	b_6^3	b_6^4	b_6^5	b_6^6
100	0.011	0.039	0.925	0.058	-0.051	-0.173	0.330	1.742
500	0.011	0.050	0.905	0.083	-0.064	-0.258	0.478	2.084
1000	0.011	0.053	0.898	0.094	-0.068	-0.294	0.540	2.227

TABLE I. Values of different WC's after RG evolution for three values of $M_{susy} = 100, 500$ and 1000 GeV.

b_i^j are the constant after running, depend on the choice of the initial scale, as shown in Table. I.

We find that the WC's with and without the RG evolution can be different by a factor of two in some cases. This implies that to have a reliable result and consistent computation one has to take into account the RG evolution of WC's.

Apart from LL type of operators, one can also have operators with different chiral structures, such as RR , LR and RL type. The operators and WC's for RR mixing can be obtained by the exchange $L \leftrightarrow R$ in Eqs. 2 and 3. LR and RL mixing cases can also be easily studied. However, in these two cases there are more stringent constraints from gluonic dipole moment operators for $B \rightarrow PP$ decays. The details have been studied in [13]. We will not discuss these two cases further.

III. DECAY AMPLITUDES FROM QCD IMPROVED FACTORIZATION

To obtain the branching ratios of $B \rightarrow PP$ decays, one needs to study the matrix elements, $\langle PP|H_{eff}|B \rangle$. The usual approach is the naive factorization method, where the hadronic matrix element can be approximated as a product of two single current matrix

elements, then it is parametrized into meson decay constant and meson-meson transition form factor.

Previous analysis of SUSY contribution to $B \rightarrow PP$ decays have been performed using the above mentioned naive factorization method. However, in the present analysis we will use the QCD improved factorization approach [2] to compute the SUSY effects to the $B \rightarrow PP$ decays. This formalism incorporates the basic elements of naive factorization approach as its leading term and perturbative QCD corrections as subleading contributions allowing one to calculate radiative corrections to the naive factorization for the hadronic two body decays of B meson.

In our case the total effective Hamiltonian for $B \rightarrow PP$ decays have two sources, the usual SM part H_{eff}^{SM} and the SUSY part H_{eff}^{susy} . We use the SM results obtained in Ref. [2]. The results for the two types of SUSY contribution from LL and RR mixing can be easily obtained once one understands the SM contributions since the operators from SUSY interactions discussed here are all strong penguin type. In the LL mixing case, the total WC's are the sum of SM WC ($C_{3..6}^{SM}$) and SUSY contributions.

$$\begin{aligned} C_3^{total} &= C_3^{SM} + C_3^{LL}, & C_4^{total} &= C_4^{SM} + C_4^{LL}, \\ C_5^{total} &= C_5^{SM} + C_5^{LL}, & C_6^{total} &= C_6^{SM} + C_6^{LL}. \end{aligned} \quad (5)$$

For RR mixing, due to the different chirality of the new operators the total WC's in the final results are replaced by $C_{3,4,5,6}^{total} = C_{3,4,5,6}^{SM} - C_{3,4,5,6}^{RR}$. The two type of mixing, LL and RR have similar contributions. Knowing how one of them affects $B \rightarrow K\pi, \pi\pi$ decays, the other can be easily estimated.

We write down the decay amplitude of $\bar{B}^0 \rightarrow \pi^+\pi^-, K^-\pi^+$ for an illustration,

$$\begin{aligned} A(\bar{B}^0 \rightarrow \pi^+\pi^-) &= \frac{G_F}{\sqrt{2}} i f_\pi (m_B^2 - m_\pi^2) F^{B \rightarrow \pi}(0) \left[V_{ub} V_{ud}^* (a_1 + a_4^u + a_{10}^u \right. \\ &\quad \left. + R_\pi (a_6^u + a_8^u)) + V_{cb} V_{cd}^* (a_4^c + a_{10}^c + R_\pi (a_6^c + a_8^c)) \right] \\ &\quad + i \frac{G_F}{\sqrt{2}} f_B f_\pi^2 \left[V_{ub} V_{ud}^* b_1 + (V_{ub} V_{ud}^* + V_{cb} V_{cd}^*) \left(b_3 + 2b_4 - \frac{1}{2} b_3^{ew} + \frac{1}{2} b_4^{ew} \right) \right] \quad (6) \\ A(\bar{B}^0 \rightarrow K^-\pi^+) &= \frac{G_F}{\sqrt{2}} i f_K (m_B^2 - m_K^2) F_0^{B \rightarrow \pi}(m_K^2) [V_{ub} V_{us}^* (a_1 + a_4^u + a_{10}^u + R_K (a_6^u + a_8^u)) \end{aligned}$$

$$\begin{aligned}
& + V_{cb} V_{cs}^* (a_4^c + a_{10}^c + R_K (a_6^c + a_8^c)) \\
& + \frac{G_F}{\sqrt{2}} i f_B f_\pi f_K (V_{ub} V_{us}^* + V_{cb} V_{cs}^*) (b_3 - \frac{1}{2} b_3^{ew})
\end{aligned} \tag{7}$$

Similarly for other $B \rightarrow K\pi, \pi\pi, KK$ modes.

Here $R_K = 2m_K^2/m_s m_b$. a_i and b_i coefficients are related to the WC's. Including the lowest α_s order corrections, a_i^q 's are given by

$$\begin{aligned}
a_1 &= C_1 + \frac{C_2}{N} \left[1 + \frac{C_F \alpha_s}{4\pi} V_K \right] + \frac{C_2}{N_c} \frac{C_F \pi \alpha_s}{N_c} H_{K\pi} \\
a_2 &= C_2 + \frac{C_1}{N} \left[1 + \frac{C_F \alpha_s}{4\pi} V_\pi \right] + \frac{C_1}{N_c} \frac{C_F \pi \alpha_s}{N_c} H_{\pi K} \\
a_4^p &= C_4^{total} + \frac{C_3^{total}}{N} \left[1 + \frac{C_F \alpha_s}{4\pi} V_K \right] + \frac{C_F \alpha_s}{4\pi} \frac{P_{K,2}^p}{N_c} + \frac{C_3^{total}}{N_c} \frac{C_F \pi \alpha_s}{N_c} H_{K\pi} \\
a_6^p &= C_6^{total} + \frac{C_5^{total}}{N} \left[1 - 6 \cdot \frac{C_F \alpha_s}{4\pi} \right] + \frac{C_F \alpha_s}{4\pi} \frac{P_{K,3}^p}{N_c} \\
a_7 &= C_7 + \frac{C_8}{N} \left[1 + \frac{C_F \alpha_s}{4\pi} (-V'_\pi) \right] + \frac{C_8}{N_c} \frac{C_F \pi \alpha_s}{N_c} (-H'_{\pi K}) \\
a_8^p &= C_8 + \frac{C_7}{N} \left[1 - 6 \cdot \frac{C_F \alpha_s}{4\pi} \right] + \frac{\alpha_{em}}{9\pi} \frac{P_{K,3}^{p,EW}}{N_c} \\
a_9 &= C_9 + \frac{C_{10}}{N} \left[1 + \frac{C_F \alpha_s}{4\pi} V_\pi \right] + \frac{C_{10}}{N_c} \frac{C_F \pi \alpha_s}{N_c} H_{\pi K} \\
a_{10}^p &= C_{10} + \frac{C_9}{N} \left[1 + \frac{C_F \alpha_s}{4\pi} V_K \right] + \frac{\alpha_{em}}{9\pi} \frac{P_{K,2}^{p,EW}}{N_c} + \frac{C_9}{N_c} \frac{C_F \pi \alpha_s}{N_c} H_{K\pi}
\end{aligned} \tag{8}$$

where $C_F = (N_c^2 - 1)/(2N_c)$, and $N_c = 3$. The quantities $V_M^{(l)}$, $H_{M_2 M_1}^{(l)}$, $P_{K,2}^p$, $P_{K,3}^p$, $P_{K,2}^{p,EW}$ and $P_{K,3}^{p,EW}$ are hadronic parameters that contain all nonperturbative dynamics. The vertex corrections V_M ($M = \pi, K$) are given by

$$V_M = 12 \ln \frac{m_b}{\mu} - 18 + \int_0^1 dx g(x) \phi_M(x) \tag{9}$$

$$V'_M = 12 \ln \frac{m_b}{\mu} - 6 + \int_0^1 dx g(1-x) \phi_M(x) \tag{10}$$

$$g(x) = 3 \left(\frac{1-2x}{1-x} \ln(x) - i\pi \right) + \left[2Li_2(x) - \ln^2(x) + \frac{2\ln(x)}{1-x} - (3 + 2i\pi) - (x \leftrightarrow 1-x) \right]. \tag{11}$$

where $\phi_M(x)$ is the leading-twist light cone distribution amplitude of light pseudoscalar meson [14]. This distribution amplitude can be expanded in Gegenbauer polynomials. We truncate this expansion at $n = 2$.

$$\phi_M(x, \mu) = 6x(1-x) \left[1 + \alpha_1^M(\mu) C_1^{(3/2)}(2x-1) + \alpha_2^M(\mu) C_2^{(3/2)(2x-1)} \right] \quad (12)$$

where $C_1^{(3/2)}(u) = 3u$ and $C_2^{(3/2)}(u) = \frac{3}{2}(5u^2 - 1)$. The distribution amplitude parameters $\alpha_{1,2}^M$ for $M = K, \pi$ are: $\alpha_1^K = 0.3$, $\alpha_2^K = 0.1$, $\alpha_1^\pi = 0$ and $\alpha_2^\pi = 0.1$. The detailed expressions can be found in [2].

For the penguin contributions, $P_{K,2}^p$, $P_{K,3}^p$, $P_{K,2}^{p,EW}$ and $P_{K,3}^{p,EW}$ are given by

$$\begin{aligned} P_{K,2}^p &= C_1 \left[\frac{4}{3} \ln \frac{m_b}{\mu} + \frac{2}{3} - G_K(s_p) \right] + C_3^{total} \left[\frac{8}{3} \ln \frac{m_b}{\mu} + \frac{4}{3} - G_K(0) - G_K(1) \right] \\ &\quad + (C_4^{total} + C_6^{total}) \left[\frac{4n_f}{3} \ln \frac{m_b}{\mu} - (n_f - 2)G_K(0) - G_K(s_c) - G_K(1) \right] \\ &\quad - 2C_{11} \int_0^1 \frac{dx}{1-x} \phi_K(x) \\ P_{K,2}^{p,EW} &= (C_1 + N_c C_2) \left[\frac{4}{3} \ln \frac{m_b}{\mu} + \frac{2}{3} - G_K(s_p) \right] - 3C_{12} \int_0^1 \frac{dx}{1-x} \phi_K(x) \\ P_{K,3}^p &= C_1 \left[\frac{4}{3} \ln \frac{m_b}{\mu} + \frac{2}{3} - \hat{G}_K(s_p) \right] + C_3^{total} \left[\frac{8}{3} \ln \frac{m_b}{\mu} + \frac{4}{3} - \hat{G}_K(0) - \hat{G}_K(1) \right] \\ &\quad + (C_4^{total} + C_6^{total}) \left[\frac{4n_f}{3} \ln \frac{m_b}{\mu} - (n_f - 2)\hat{G}_K(0) - \hat{G}_K(s_c) - \hat{G}_K(1) \right] - 2C_{11} \\ P_{K,3}^{p,EW} &= (C_1 + N_c C_2) \left[\frac{4}{3} \ln \frac{m_b}{\mu} + \frac{2}{3} - \hat{G}_K(s_p) \right] - 3C_{12} \end{aligned} \quad (13)$$

with

$$\begin{aligned} G_K(s) &= \int_0^1 dx G_K(s - i\epsilon, 1-x) \phi_K(x) \\ \hat{G}_K(s) &= \int_0^1 dx G_K(s - i\epsilon, 1-x) \phi_p^K(x) \\ G_K(s, x) &= -4 \int_0^1 du u(1-u) \ln[s - u(1-u)x] \end{aligned} \quad (14)$$

where $\phi_p(x) = 1$.

The hard spectator contributions to the coefficients a_i 's are parametrized in terms of a single (complex) quantity $H'_{M_1 M_2}$ which suffers from large theoretical uncertainties related to the regularization of the divergent endpoint integral. Following [2] we use $H_{\pi K} = H_{KK} = 0.99$ at the scale $\mu = m_b$ and

$$H'_{\pi K} = H_{\pi K}, \quad H_{K\pi} = R_{\pi K} H_{\pi K}. \quad (15)$$

All scale-dependent quantities for hard spectator contributions are evaluated at $\mu_h = \sqrt{\Lambda_h m_b}$ with $\Lambda_h = 0.5$ GeV.

Terms containing the coefficients b_i and b_i^{ew} are from annihilation contributions. The annihilation coefficients are

$$\begin{aligned}
b_1 &= \frac{C_F}{N_c^2} C_2 A_1^i, & b_3 &= \frac{C_F}{N_c^2} [C_3^{total} A_1^i + C_5^{total} (A_3^i + A_3^f) + N_c C_6^{total} A_3^f] \\
b_2 &= \frac{C_F}{N_c^2} C_2 A_1^i, & b_4 &= \frac{C_F}{N_c^2} [C_4^{total} A_1^i + C_6^{total} A_2^i] \\
b_3^{ew} &= \frac{C_F}{N_c^2} [C_9 A_1^i + C_7 (A_3^i + A_3^f) + N_c C_8 A_3^f] \\
b_4^{ew} &= \frac{C_F}{N_c^2} [C_{10} A_1^i + C_8 A_2^i].
\end{aligned} \tag{16}$$

with

$$\begin{aligned}
A_1^i &= A_2^i = \pi \alpha_s \left[18 \left(X_A - 4 + \frac{\pi^2}{3} \right) + 2 r_\chi^2 X_A^2 \right] \\
A_3^f &= 12 \pi \alpha_s r_\chi^2 (2 X_A^2 - X_A)
\end{aligned} \tag{17}$$

where $r_\chi = 2\mu_h/m_b$, $X_A = \int_0^1 dy/y$ parameterizes the divergent endpoint integrals. We use $X_A = \ln(m_B/\Lambda_h)$. All scale dependent quantities for annihilation contributions are evaluated at μ_h .

In the QCD improved factorization method the weak annihilation contributions are power suppressed as Λ_{QCD}/m_b and hence do not appear in the factorization formula. Apart from this, they also show end-point singularities even at twist-two order in the light-cone expansion of the final state light mesons and therefore can not be calculated systematically in the context of hard scattering approach. One can bypass this problem, by treating these different end-point singularities as a phenomenological parameters. But this induces model dependence and numerical uncertainties in the calculation.

Using the above technique we compute the different two-body branching ratios of B mesons within the framework of SUSY and compare the calculated results with the experimental data to constrain the different flavor changing parameters of SUSY. The experimental branching ratios used in this analysis are listed in Table II. We average the data from CLEO,

BaBar, Belle B -factories as their results are uncorrelated. To impose the limit on these flavor changing parameters we require that the theoretically computed branching ratios should not deviate from the experimental measurement by 2σ . If the experimental branching ratio has only upper limit, we select the most stringent one from the experimental data. It is clear from Table II that for $B \rightarrow \pi^0 \pi^0$ and $B \rightarrow KK$ modes have only the 90% C.L. upper limit.

TABLE II. The branching ratios for $B \rightarrow PP$ in units of 10^{-6} .

Branching ratio and CP asymmetries	Cleo [15]	Belle [16]	Babar [17]	Averaged Value
$Br(B_u \rightarrow \pi^- \bar{K}^0)$	$18.8^{+3.7+2.1}_{-3.3-1.8}$	$22.0 \pm 1.9 \pm 1.1$	$17.5^{+1.8}_{-1.7} \pm 1.3$	19.7 ± 1.5
$Br(B_u \rightarrow \pi^0 K^-)$	$12.9^{+2.4+1.2}_{-2.2-1.1}$	$12.8 \pm 1.4^{+1.4}_{-1.0}$	$12.8^{+1.2}_{-1.1} \pm 1.0$	12.8 ± 1.1
$Br(B_d \rightarrow \pi^+ K^-)$	$18.0^{+2.3+1.2}_{-2.1-0.9}$	$18.5 \pm 1.0 \pm 0.7$	$17.9 \pm 0.9 \pm 0.7$	18.2 ± 0.8
$Br(B_d \rightarrow \pi^0 \bar{K}^0)$	$12.8^{+4.0+1.7}_{-3.3-1.4}$	$12.6 \pm 2.4 \pm 1.4$	$10.4 \pm 1.5 \pm 0.8$	11.2 ± 1.4
$Br(B_u \rightarrow \pi^- \pi^0)$	$4.6^{+1.8+0.6}_{-1.6-0.7}$	$5.3 \pm 1.3 \pm 0.5$	$5.5^{+1.0}_{-0.9} \pm 0.6$	5.3 ± 0.8
$Br(B_d \rightarrow \pi^+ \pi^-)$	$4.5^{+1.4+0.5}_{-1.2-0.4}$	$4.4 \pm 0.6 \pm 0.3$	$4.7 \pm 0.6 \pm 0.2$	4.6 ± 0.4
$Br(B_d \rightarrow \pi^0 \pi^0)$	$< 4.4(90\% \text{C.L.})$	$< 4.4(90\% \text{C.L.})$	$< 3.6(90\% \text{C.L.})$	$< 3.6(90\% \text{C.L.})$
$Br(B_u \rightarrow K^- K^0)$	$< 3.3(90\% \text{C.L.})$	$< 3.4(90\% \text{C.L.})$	$< 1.3(90\% \text{C.L.})$	$< 1.3(90\% \text{C.L.})$
$Br(B_d \rightarrow K^- K^+)$	$< 0.8(90\% \text{C.L.})$	$< 0.7(90\% \text{C.L.})$	$< 0.6(90\% \text{C.L.})$	$< 0.6(90\% \text{C.L.})$
$Br(B_d \rightarrow \bar{K}^0 K^0)$	$< 3.3(90\% \text{C.L.})$	$< 3.2(90\% \text{C.L.})$	$< 7.3(90\% \text{C.L.})$	$< 3.2(90\% \text{C.L.})$

For our numerical calculations, we use $m_b(m_b) = 4.2$ GeV for the b quark mass, $m_c(m_b) = 1.3 \pm 0.2$ GeV, $m_s(2 \text{ GeV}) = 110.0 \pm 0.25$ MeV, $(m_u + m_d)(2\text{GeV}) = 9.1 \pm 2.1$ MeV. For the decay constants and form factors, we use $f_\pi = 0.131$ GeV, $f_K = 0.160$ GeV, $f_B = 0.180$ GeV, $F^{B \rightarrow \pi} = 0.28$, $r_{\pi K} \simeq \frac{F^{B \rightarrow K} f_\pi}{F^{B \rightarrow \pi} f_K} = 0.9$ [2,18]. For the CKM matrix elements, we fix $\lambda = 0.2196$, and take the central values of $|V_{cb}| = 0.0412 \pm 0.002$, $|\frac{V_{ub}}{V_{cb}}| = 0.087 \pm 0.018$ [18]. We fix the CP violating phase γ to 53.6° from global fit-

ting of CKM parameters. With the above input parameters, the SM contributions are fixed. However, in SUSY the branching ratios depend on several parameters, such as $(\delta_{j3})_{LL}$, the squark mass $m_{\tilde{q}}$, and the ratio $x = m_{\tilde{g}}^2/m_{\tilde{q}}^2$. We treat $m_{\tilde{q}}$ and x as free parameters and constrain $(\delta_{j3})_{LL}$ from the available experimental data. Our main aim will be to obtain limits on the complex plane of the flavor changing parameters $(\delta_{j3})_{LL}$ for a given x and the squark mass. Otherwise mentioned, throughout our analysis we will use 100 GeV for squark mass. Constraints on $(\delta_{j3})_{LL}$ for other values of $m_{\tilde{q}}$ can be obtained by rescaling the constraint by $(m_{\tilde{q}}/100 \text{ GeV})^2$.

In the theoretical computations of the branching ratios, there are many sources of uncertainties, mainly arising from different form factors, CKM matrix elements, the annihilation contribution and other hadronic parameters of the QCD improved factorization methods. We have taken the default values of the above quantities following [2] to get the central values of the theoretically calculated branching ratios. However, the results may change if one varies any of the above parameters within their allowed range. To take into account this fact we conservatively allow an extra 50% variation in the theoretically calculated branching ratios from their default values. In the later section we will discuss more on these uncertainties. The input values chosen here are for an illustration. The main issue of our analysis is to show that $B \rightarrow PP$ can provide comparable or even better constraints in certain area of SUSY parameter space compared with other well known rare processes for B mesons, like $b \rightarrow s\gamma$, $B \rightarrow \rho\gamma$, and the mixing parameters Δm_{B_s} and Δm_{B_d} .

IV. $B \rightarrow PP(\Delta S = -1)$, $B \rightarrow S\gamma$ AND $B_S^0 - \bar{B}_S^0$ MIXING

In this section we study constraints on the parameter $(\delta_{23})_{LL}$ from $B \rightarrow K\pi$ and compare with the constraint from $b \rightarrow s\gamma$. We also comment on how $B_s^0 - \bar{B}_s^0$ mixing can provide information of FCNC parameters in SUSY. Since we are primarily interested in constraining the flavor changing parameter $(\delta_{23})_{LL}$, we will present our results on the complex plane of the $(\delta_{23})_{LL}$ for a given value of $m_{\tilde{q}}$ and x .

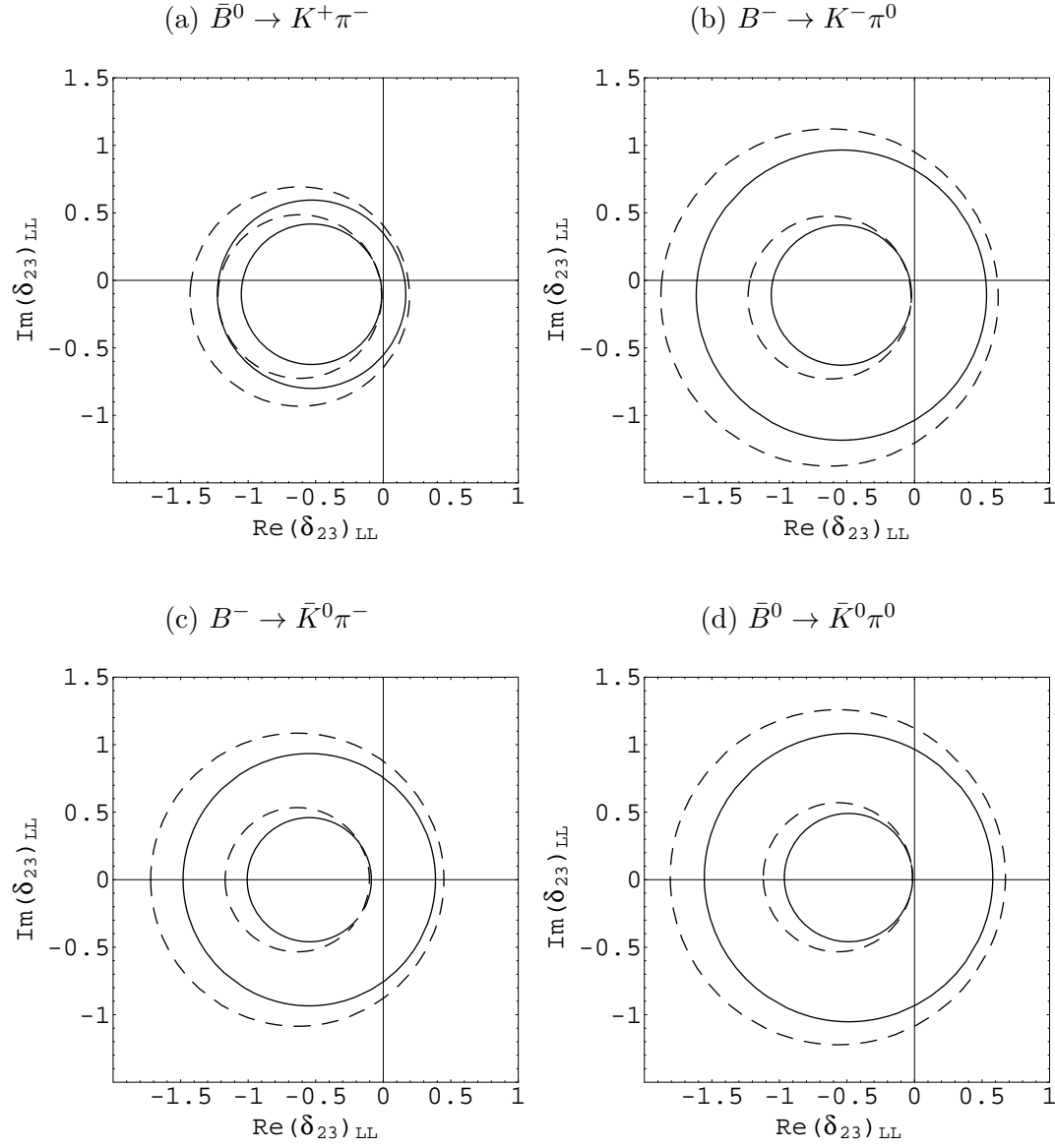


FIG. 1. The 2σ allowed region on $(\delta_{23})_{LL}$ complex plane from $B \rightarrow K\pi$ with $m_{\bar{q}} = 100$ GeV. The solid and dashed bands are the allowed regions corresponding to $x = 1$ and 4 respectively.

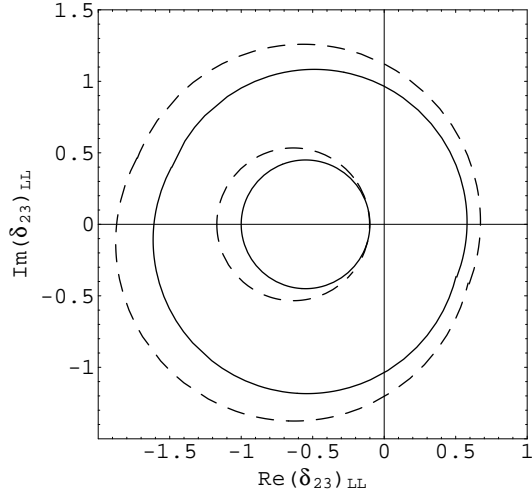


FIG. 2. Combined 2σ allowed region on $(\delta_{23})_{LL}$ complex plane obtained from four $B \rightarrow K\pi$ modes as shown in Figure 1. Other notations are same as Figure 1.

In Figure 1 we show 2σ allowed bands on the $(\delta_{23})_{LL}$ complex plane for two representative values of $x = 1$ (solid line) and 4 (dashed line) for the squark mass set at 100 GeV . From the above Figure with $m_{\tilde{q}} = 100 \text{ GeV}$, it is clear that the four different decay channels of B into $K^+\pi^-$, $K^-\pi^0$, $\bar{K}^0\pi^-$, $\bar{K}^0\pi^0$ give almost similar limits and the allowed ranges are almost smaller than 1 on the $(\delta_{23})_{LL}$ complex plane. There is no significant change in the obtained bound even when x varies in the range $0.5 \sim 10$. We finally combine the results obtained from these four branching ratios and display it in Figure 2. We see that the flavor changing parameter $(\delta_{23})_{LL}$ is constrained.

If the squark mass $m_{\tilde{q}}$ is different than the value 100 GeV used here, one can obtain the corresponding constraint on $(\delta_{23})_{LL}$ by multiplying a scaling factor $m_{\tilde{q}}^2/(100 \text{ GeV})^2$ on $(\delta_{23})_{LL}$. We would like to point out, however, that when making such a rescaling one should be cautious about the applicability of the mass insertion method used to obtain the effective Hamiltonian. One should only apply the results to regions where $(\delta_{23})_{LL}$ is not larger than of order one. Since the constraint on $(\delta_{23})_{LL}$ is already of order one for $m_{\tilde{q}}$ about 100 GeV , for a larger $m_{\tilde{q}}$ $B \rightarrow PP$ give weak constraints on the flavor changing parameters.

We now compare the above constraints with that from $b \rightarrow s\gamma$. We take the current

experimental world average result $Br(B \rightarrow X_s \gamma) = (3.41 \pm 0.36) \times 10^{-4}$ [19] from CLEO, ALEPH, Belle and Babar. This process is another rare process which is sensitive to new physics with $\Delta S = -1$ and has been used to constrain new physics beyond the SM.

The branching ratio of $b \rightarrow s \gamma$ is given by [20,21]

$$Br(B \rightarrow X_s \gamma) = Br(B \rightarrow X e \bar{\nu}_e) \frac{|V_{ts}^* V_{tb}|^2}{|V_{cb}|^2} \frac{6\alpha_{em}}{\pi g(m_c/m_b)\eta} |c_{12}(m_b)|^2, \quad (18)$$

where $c_{12}(m_b) = c_{12}^{SM}(m_b) + c_{12}^{susy}(m_b)$, $g(z) = 1 - 8z^2 + 8z^6 - z^8 - 24z^4 \ln(z)$, and $\eta = 1 - 2f(r, 0, 0)\alpha_s(m_b)/3\pi$ with $f(r, 0, 0) = 2.41$ [21]. The running of the supersymmetric WC's $c_{11,12}^{susy}$ are given by [22]

$$c_{11}^{susy}(\mu) = \eta c_{11}^{susy}(M_{susy}), \quad c_{12}^{susy}(\mu) = \eta^2 c_{12}^{susy}(M_{susy}) + \frac{8}{3}(\eta - \eta^2) c_{11}^{susy}(M_{susy}), \quad (19)$$

where $\eta = (\alpha_s(M_{susy})/\alpha_s(m_t))^{2/21}(\alpha_s(m_t)/\alpha_s(m_b))^{2/23}$, with

$$\begin{aligned} c_{11}^{susy}(M_{susy}) &= \frac{-\alpha_s \pi (\delta_{j3})_{LL}}{m_{\tilde{q}}^2 \sqrt{2} G_F V_{tb} V_{tq}^*} \left(-\frac{1}{3} M_3(x) - 3M_4(x) \right) \\ c_{12}^{susy}(M_{susy}) &= \frac{-\alpha_s \pi (\delta_{j3})_{LL}}{m_{\tilde{q}}^2 \sqrt{2} G_F V_{tb} V_{tq}^*} \left(-\frac{1}{3} \frac{8}{3} M_3(x) \right) \end{aligned} \quad (20)$$

The functions $M_{3,4}(x)$ are defined in Ref. [6]. Here we use the leading order result for $b \rightarrow s \gamma$. The use of the NLO result [23] will change the LO results by about 10%, which will not affect our main conclusion.

The 2σ constraints on $(\delta_{23})_{LL}$ complex plane from $b \rightarrow s \gamma$ for two different values of $x = 1$ and 4 are shown in Figure 3. From this figure we see that as x increases the limit on $(\delta_{23})_{LL}$ from $b \rightarrow s \gamma$ become weaker.

It was thought that $b \rightarrow s \gamma$ gives the strongest limit on the parameter $(\delta_{23})_{LL}$. However, in our analysis we find that in certain region of the parameter space the bounds obtained from $B \rightarrow K \pi$ are stronger than the limit obtained from $b \rightarrow s \gamma$. From Figure 4 we see that for $x = 8$ constraints from $B \rightarrow K \pi$ provide slightly better constraints than that from $b \rightarrow s \gamma$. We find that for x less than 8, the constraints obtained from $B \rightarrow PP$ are not as strong as that from $b \rightarrow s \gamma$. But for x larger than 8, the constraints from $B \rightarrow PP$ is more stringent.

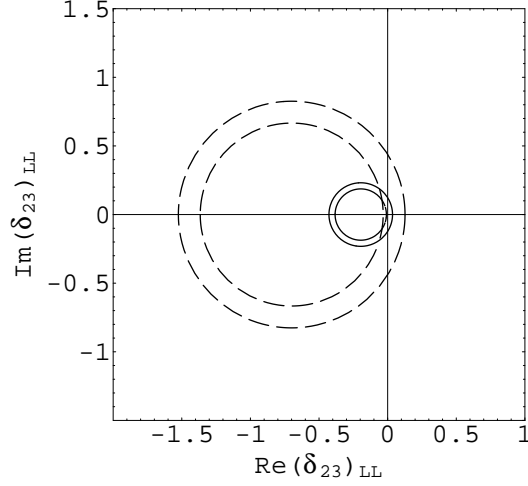


FIG. 3. The 2σ allowed bands obtained from $b \rightarrow s\gamma$ on the complex $(\delta_{23})_{LL}$ plane with $m_{\tilde{q}} = 100$ GeV. Other notations are same as Figure 1.

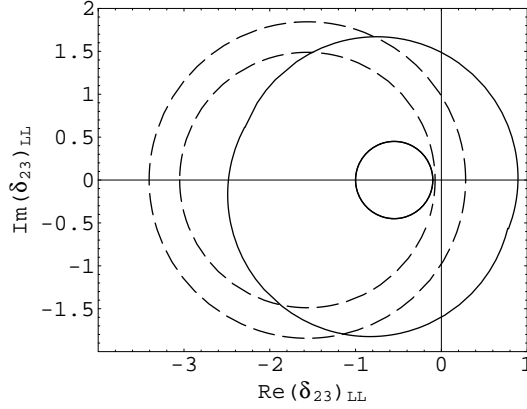


FIG. 4. Combined 2σ allowed region on $(\delta_{23})_{LL}$ complex plane obtained from $B \rightarrow K\pi$ (solid band) and $b \rightarrow s\gamma$ (dashed band) for $x = 8$ with $m_{\tilde{q}} = 100$ GeV.

One can easily understand the above results from the x dependence of SUSY contributions to $B \rightarrow K\pi$ and $b \rightarrow s\gamma$. From Eq. 7, we find that the SUSY contributions mainly appear in parameters a_4 and a_6 through $C_{3,4,5,6}^{total}$.

$$a^{susy} = a_4^{susy} + a_6^{susy} = C_4^{LL} + \frac{C_3^{LL}}{N} + R_{\pi,K}(C_6^{LL} + \frac{C_5^{LL}}{N}). \quad (21)$$

We have checked numerically that the other contributions in Eq. 7 from SUSY interactions are small.

The parameter a^{susy} linearly depends on $(\delta_{j3})_{LL}/m_{\tilde{q}}^2$ and depends on x in a complicated

but known form which we indicate as $a^{susy} = a^{susy}(x)$. One can easily study how experimental data may constrain the parameter $(\delta_{j3})_{LL}/m_{\tilde{q}}^2$ as a function of x by studying the behavior of

$$R(PP) = \frac{a^{susy}(x)}{a^{susy}(1)}. \quad (22)$$

The above function shows the behavior of the SUSY contribution with x normalized with the value at $x = 1$. In Figure 5, we show the behavior of $R(PP)$ as a function of x by the dark solid line. From the figure we see that $R(PP)$ has a zero value at $x \simeq 0.37$. This implies that for $x \simeq 0.37$, no constraint on $(\delta_{23})_{LL}$ from $B \rightarrow PP$. In the neighborhood of this region $b \rightarrow s\gamma$ certainly give a better bound. For x in the range $1 \sim 10$, $R(PP)$ varies very slowly with x . This almost flat behavior of $R(PP)$ makes the bound on $(\delta_{23})_{LL}$ to remain nearly unchanged within this range of x .

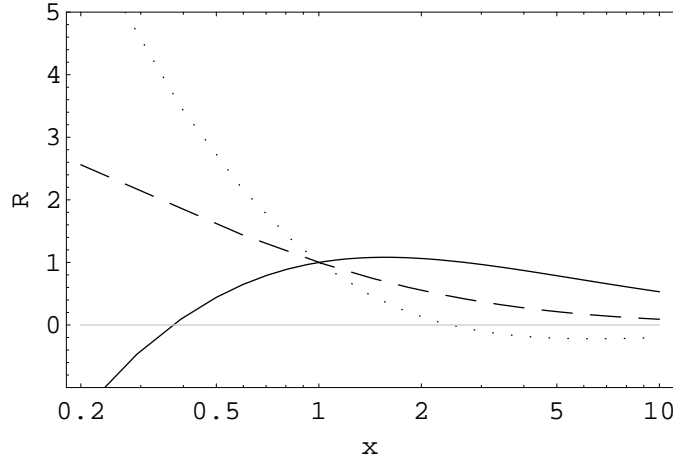


FIG. 5. $R(PP)$, $R(q\gamma)$ and $R(B_{d,s}^0 - \bar{B}_{d,s}^0)$ as functions of x . The solid, dashed and dotted lines correspond to $R(PP)$, $R(q\gamma)$, and $R(B_{d,s}^0 - \bar{B}_{d,s}^0)$, respectively.

While for $b \rightarrow s\gamma$, the SUSY contribution has a different x dependence. In Figure 5 we show the variation of

$$R(q\gamma) = \frac{c_{12}^{susy}(x)}{c_{12}^{susy}(1)}, \quad (23)$$

as a function of x by the dashed line. We see that $R(q\gamma)$ decreases when x increases. This means, for a given $m_{\tilde{q}}$, the constraint on $(\delta_{23})_{LL}$ becomes weaker as x increases. At certain

value of x , $B \rightarrow K\pi$ give better bounds than $b \rightarrow s\gamma$. Numerically we find that when x is larger than 8, $B \rightarrow K\pi$ give better constraints on $(\delta_{23})_{LL}$ than $b \rightarrow s\gamma$.

We now comment on the implications of $q - \tilde{q} - \tilde{g}$ interactions on $B_s^0 - \bar{B}_s^0$ mixing. The effective Hamiltonian for this process is given by [6]

$$H_{eff} = -C_m O_m , \quad (24)$$

$$C_m = \frac{\alpha_s^2}{216m_{\tilde{q}}^2} [24x f_6(x) + 66\tilde{f}_6(x)] (\delta_{j3})_{LL}^2 , \quad (25)$$

$$O_m = \bar{s}_L^\alpha \gamma_\mu b_L^\alpha \bar{s}_L^\beta \gamma_\mu b_L^\beta \quad (26)$$

The functions $f_6(x)$ and $\tilde{f}_6(x)$ are given by:

$$f_6(x) = \frac{6(1+3x)\ln(x) + x^3 - 9x^2 - 9x + 17}{6(1-x)^5} , \quad (27)$$

$$\tilde{f}_6(x) = \frac{6x(1+x)\ln(x) - x^3 - 9x^2 + 9x + 1}{3(1-x)^3} . \quad (28)$$

After RG evolution we get the WC at m_b scale [24]:

$$C_m(m_b) = \eta_1 C_m(M_{susy}) , \quad (29)$$

$$\eta_1 = \left(\frac{\alpha_s(m_t)}{\alpha_s(m_b)} \right)^{6/23} \left(\frac{\alpha_s(M_{susy})}{\alpha_s(m_t)} \right)^{6/21} , \quad (30)$$

the total ΔM_{B_s} is given by $\Delta M_{B_s} = 2|M_{12}^{SM} + M_{12}^{susy}|$ with $M_{12}^{susy} = \eta_1 (C_m/3) M_{B_s} B_{B_s} f_{B_s}^2$. The SM contribution M_{12}^{SM} is given by [25], and M_{12}^{susy} contains phase from parameter $(\delta_{j3})_{LL}^2$. At present we have only stringent lower bound on ΔM_{B_s} which is 14.4 ps^{-1} at the 95% C.L. [26]. Using previously obtained constraints one can obtain the allowed range for ΔM_{B_s} with SUSY contributions. In our numerical calculation we use [18] $\xi \equiv \sqrt{B_{B_s}}/f_{B_s} \sqrt{B_{B_d}}f_{B_d} = 1.16 \pm 0.05$ and $\sqrt{B_{B_d}}f_{B_d} = 230 \pm 40 \text{ MeV}$.

We find that $B \rightarrow K\pi$ and $b \rightarrow s\gamma$ data do not constrain ΔM_{B_s} significantly in a large part of the parameter space allowing ΔM_{B_s} to be much larger than the present lower bound. If future experiments can measure ΔM_{B_s} of the order or less than $\sim 48 \text{ ps}^{-1}$, which is the limit LHCb can reach, then, one would obtain a much stronger limit on $(\delta_{23})_{LL}$ for $x = 1$ and 4 as shown in Figure 6. However we still find that there are regions where

$B \rightarrow K\pi$ and $b \rightarrow s\gamma$ give better constraints. To see in which area of parameter space, the SUSY contributions to ΔM_{B_s} become negligible, we study the behavior of relative SUSY contribution, $R(B_s^0 - \bar{B}_s^0) = C_m(x)/C_m(1)$ as a function of x . In Figure 5 we show the variation of $R(B_s^0 - \bar{B}_s^0)$ as a function of x by the dotted lines. we see that at $x = 2.43$ SUSY contribution to ΔM_{B_s} becomes zero and no constraint on $(\delta_{23})_{LL}$ can be obtained. In regions around $x = 2.43$, $B \rightarrow K\pi$ and $b \rightarrow s\gamma$ can give better constraints even if we assume that the future experiment will measure a ΔM_{B_s} less than 48 ps^{-1} .

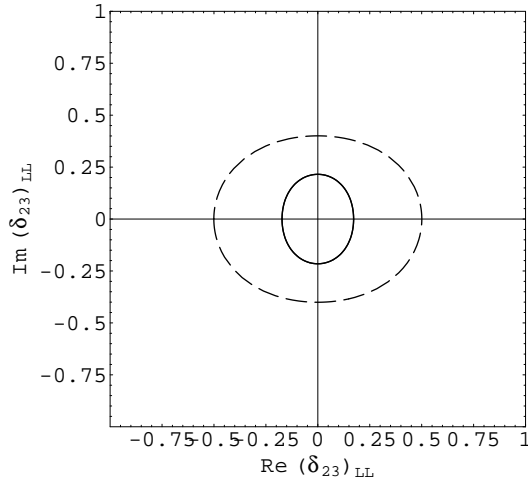


FIG. 6. The allowed areas (areas inside each curve are excluded if ΔM_{B_s} is larger than 48 ps^{-1}) with solid and dashed boundaries corresponding to $x = 1$ and 4 respectively on the complex plane of $(\delta_{23})_{LL}$.

V. $B \rightarrow PP(\Delta S = 0)$, $B \rightarrow \rho\gamma$ AND $B_D - \bar{B}_D$ MIXING

In this section we discuss constraints on SUSY interactions from following processes: $B \rightarrow \pi\pi, KK$, $B \rightarrow \rho\gamma$ and ΔM_{B_d} . Constraints obtained from $B \rightarrow \pi\pi$ and $B \rightarrow KK$ are shown in Figure 7. We find that the constraints on $(\delta_{13})_{LL}$ are better than $(\delta_{23})_{LL}$ obtained from $B \rightarrow K\pi$ decays. The strongest one is obtained from $B^- \rightarrow K^- K^0$.

Although $B \rightarrow \rho\gamma$ has not been measured, the experimental upper bound from BaBar $Br(B^0 \rightarrow \rho^0\gamma) \leq 1.4 \times 10^{-6}$ at the 90%C.L. [27] has been used to obtain a constraint on

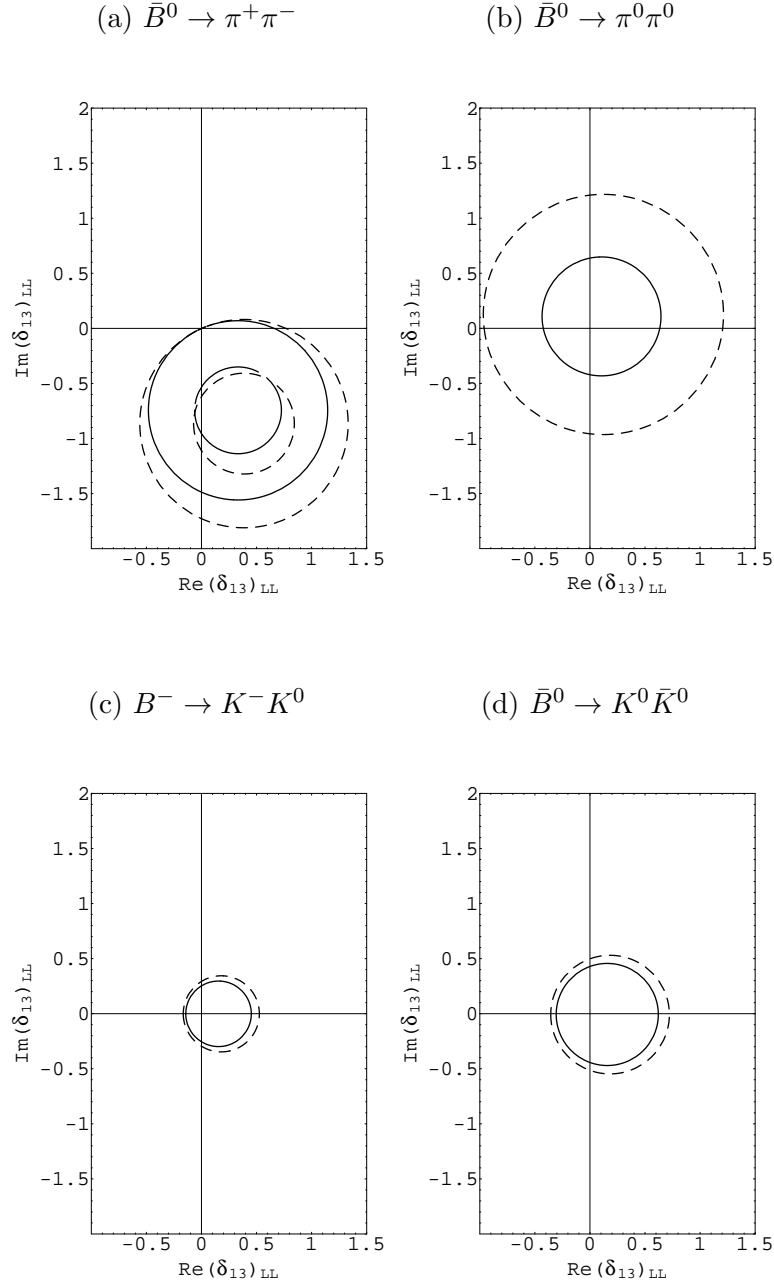


FIG. 7. The constraint on $(\delta_{13})_{LL}$ from $B \rightarrow \pi\pi$, $B \rightarrow K\bar{K}$. For $B \rightarrow \pi^+\pi^-$ are 2σ allowed region while for $B \rightarrow \pi^0\pi^0$, $B \rightarrow K^-K^0$ and $B \rightarrow K^0\bar{K}^0$ is the limits with 90%C.L. The solid and dashed bands (a) and circles ((b)-(d)) are the allowed regions corresponding to $x = 1$ and 4 respectively.

$(\delta_{13})_{LL}$. The decay width $\Gamma(B \rightarrow \rho\gamma)$ is given by:

$$\Gamma(B \rightarrow \rho\gamma) = \frac{\alpha_{em}}{32\pi^4} G_F^2 |V_{tb}|^2 |V_{td}^*|^2 |F^{B \rightarrow \rho}(0)|^2 |c_{12}(m_b)|^2 (m_b^2 + m_d^2) \frac{(m_B^2 - m_\rho^2)^3}{m_B^3} \quad (31)$$

We use the form factor calculated by T. Huang *et al.* in Ref. [28], $F^{B \rightarrow \rho^0} = 0.237 \pm 0.035$. The constraints on $(\delta_{13})_{LL}$ for $x = 1$ and 4 are shown in Figure 8. Comparing the constraints obtained from $B \rightarrow \pi\pi, KK$ with $B \rightarrow \rho\gamma$ we find that similar to the discussions in the previous section, when x becomes larger the constraint from $B^- \rightarrow K^- K^0$ become relatively better than $B \rightarrow \rho\gamma$, numerically for the strongest case $B^- \rightarrow K^- K^0$, this occurs at x about 6.

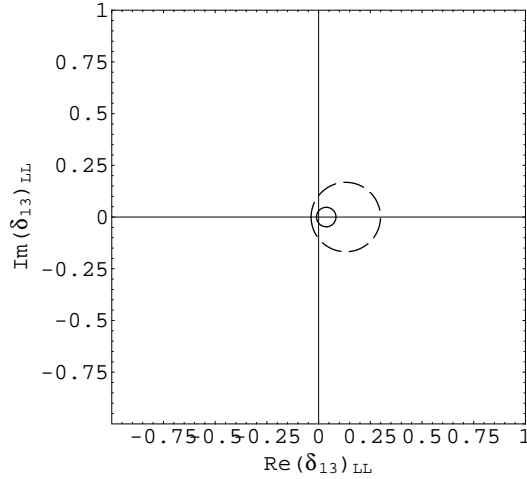


FIG. 8. The constraint of $(\delta_{13})_{LL}$ from $B \rightarrow \rho\gamma$. The allowed area marked by solid and dashed line correspond to $x = 1$ and 4 respectively.

We now turn to constraint from ΔM_{B_d} . This quantity has been experimentally well measured with the world average value [18] $0.489 \pm 0.008 \text{ ps}^{-1}$. However, the theoretical calculation has uncertainty from $\sqrt{B_d} f_{B_d}$, which is $230 \pm 40 \text{ MeV}$. The results are shown in Figure 9. It can be seen that ΔM_{B_d} provides a much stronger constraint on $(\delta_{13})_{LL}$ compared with the constraint on $(\delta_{23})_{LL}$ from ΔM_{B_s} . In a large part of the parameter space the branching ratios $B \rightarrow \pi\pi$, $B \rightarrow K\bar{K}$ provide weaker constraints on $(\delta_{13})_{LL}$ unless x is close to 2.43 where SUSY contribute to ΔM_{B_d} is zero as can be seen from Figure 5. In the region around $x = 2.43$ $B \rightarrow K^- K^0$ and $B \rightarrow \rho\gamma$ give better bounds.

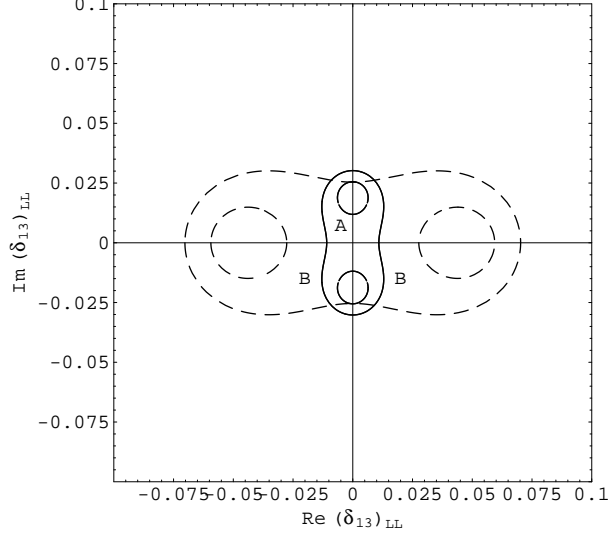


FIG. 9. The areas marked by “A” and “B” on the complex $(\delta_{23})_{LL}$ plane represent 2σ allowed regions for $x = 1$ and 4 respectively obtained from $B_d - \bar{B}_d$ mixing.

VI. CONSTRAINTS ON $(\delta_{IJ})_{RR}$

In the previous discussions, we have concentrated on constraints on $(\delta_{ij})_{LL}$. We now discuss constraints on $(\delta_{ij})_{RR}$. Due to the different chirality of the new operators the total WC's, in the theoretical expressions for $B \rightarrow PP$, are replaced by $C_{3,4,5,6}^{total} = C_{3,4,5,6}^{SM} - C_{3,4,5,6}^{RR}$, where $C_{3,4,5,6}^{RR}$ have the same form as for $C_{3,4,5,6}^{LL}$ in Eq. 3 with $(\delta_{ij})_{LL}$ replaced by $(\delta_{ij})_{RR}$.

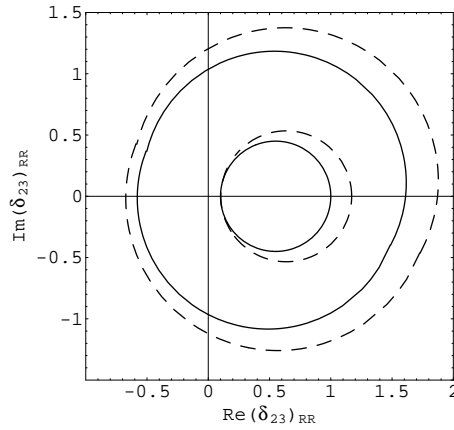


FIG. 10. Combined $(\bar{B}^0 \rightarrow K^+\pi^-, \bar{K}^0\pi^0)$ and $(B^- \rightarrow K^-\pi^0, \bar{K}^0\pi^-)$ constraints on $(\delta_{23})_{RR}$ with $m_{\tilde{q}} = 100$ GeV.

In Figure 10, we present the combined ($\bar{B}^0 \rightarrow K^+\pi^-$, $\bar{K}^0\pi^0$) and ($B^- \rightarrow K^-\pi^0$, $\bar{K}^0\pi^-$) constraints on $(\delta_{23})_{RR}$. The allowed ranges are the same but as a mirror reflection in complex plane of $(\delta_{ij})_{RR}$ compared with that of $(\delta_{ij})_{LL}$.

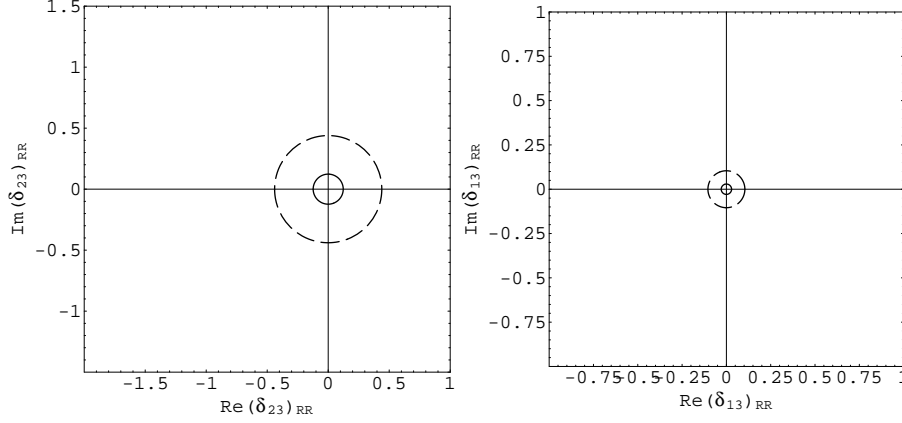


FIG. 11. $b \rightarrow s\gamma$ and $B \rightarrow \rho\gamma$ on $(\delta_{23})_{RR}$ with $m_{\tilde{q}} = 100$ GeV.

In $b \rightarrow s\gamma$ and $B \rightarrow \rho\gamma$ cases, because of different chirality in operators, the Wilson coefficient c_{12}^{susy} is separated from the SM contribution c_{12}^{SM} . One needs to replace $|c_{12}(m_b)|^2$ in Eq. 18 and Eq. 31 by $|c_{12}(m_b)|^2 = |c_{12}^{SM}|^2 + |c_{12}^{susy}|^2$. The allowed ranges are shown in Figure 11. We see that they are different than those shown in Figures 3 and 8. It is clear that the allowed ranges of $(\delta_{ij})_{RR}$ are constrained to be smaller than $(\delta_{ij})_{LL}$.

$B_{d,s} - \bar{B}_{d,s}$ mixing also constrain $(\delta_{ij})_{RR}$. In this case one just needs to replace $(\delta_{ij})_{LL}$ in Eq. 25 by $(\delta_{ij})_{RR}$ and $Q_m = \bar{s}_L^\alpha \gamma_\mu b_L^\alpha \bar{s}_L^\beta \gamma_\mu b_L^\beta$ by $\tilde{Q}_m = \bar{s}_R^\alpha \gamma_\mu b_R^\alpha \bar{s}_R^\beta \gamma_\mu b_R^\beta$. Since $\langle B^0 | Q_m | \bar{B}^0 \rangle = \langle B^0 | \tilde{Q}_m | \bar{B}^0 \rangle$, the constraints on $(\delta_{ij})_{RR}$ from $\Delta m_{B_{d,s}}$ are the same as in Figures 6 and 9.

VII. CONCLUSIONS

In this paper we studied the constraints on the SUSY flavor changing parameters $(\delta_{13})_{LL,RR}$ and $(\delta_{23})_{LL,RR}$ from rare hadronic $B \rightarrow PP$ decays. We improved the calculations by two folds. Firstly, all the relevant Wilson coefficients are computed at M_{susy} and then evolved down to lower scale $\mu = m_b$ using Renormalization Group Equation. Secondly, we calculated the two body hadronic B decays using QCD improved factorization method.

We found that the values of the Wilson coefficients do change significantly under this evolution which in turn affect the theoretical computation of B decays. The constraints obtained are compared with radiative $b \rightarrow s\gamma$ and $B \rightarrow \rho\gamma$ decays, and $\Delta M_{B_{d,s}}$.

We found that each of the different processes discussed can provide interesting constraints on the SUSY flavor changing parameters within certain parameter space. For $(\delta_{23})_{LL,RR}$ we found that as long as $x \leq 7$, $b \rightarrow s\gamma$ provides the most stringent limit, however, for $x \geq 8$, $B \rightarrow K\pi$ give better constraints. For $(\delta_{13})_{LL,RR}$ we observed ΔM_{B_d} provides a better bound, but for x around 2.43, the bound becomes weaker. In this region, $B \rightarrow K^- K^0$ and $B \rightarrow \rho\gamma$ can give stronger constraint.

Before we conclude, we would like to comment on the possible theoretical uncertainties arising from different form factors, CKM elements, the hard spectator interactions and also from annihilation contributions in QCD improved factorization scheme. As we have already mentioned earlier that these hard spectator interactions and annihilation contributions in QCD improved factorization method suffer from endpoint singularities and these singularities have been treated as a phenomenological parameters inducing model dependence and additional source of numerical uncertainties. However, the exact estimations of these uncertainties are not yet known. The uncertainties in the different form factors can change the theoretical results by about 40%. We think that the overall uncertainty could be around 50%. So, in our theoretical calculations we have taken into account this 50% uncertainty to obtain the limits. In our calculations we also fixed the SM phase γ to be 53.6° . When SUSY contributions are included, the γ phase will differ from its SM value. Allowing γ to vary will also change the details of the numerical results.

However our main objective here was to explore all possible $B \rightarrow PP$ decays within the context of SUSY and show how in different regions of parameter space the different decay modes can constrain the FCNC parameters. The generic feature of our analysis will not change significantly by the above mentioned different uncertainties. A coherent study of different processes involving B -mesons carried out here can serve to provide detailed information about the SUSY FCNC parameters. We hope in future with the improved

theoretical calculations and data will provide a better understanding of SUSY flavor changing interactions.

ACKNOWLEDGMENTS

This work is partially supported by the ROC National Science Council under the grant NSC 90-2811-M-002-054, NSC 90-2112-002-058 and by the ROC Ministry of Education Academic Excellence Project 89-N-FA01-1-4-3.

REFERENCES

- [1] H. P. Nilles, *Phys. Rep.* **110**, 1 (1984); H. E. Haber and G. L. Kane, *Phys. Rep.* **117**, 75 (1985).
- [2] M. Beneke et al., *Phys. Rev. Lett.* **83**, 1914 (1999); *Nucl. Phys.* **B591**, 313 (2000).
- [3] Y.-Y. Keum, H.-n. Li and I. Sanda, *Phys. Lett.* **B504**, 6 (2001); *Phys. Rev. D* **63**, 054008 (2001).
- [4] D. S. Du et al., hep-ph/0108141; D. -S. Du, D. -S. Yang and G. -H. Zhu, *Phys. Rev. D* **64**, 014036 (2001); *Phys. Lett.* **B509**, 263 (2001).
- [5] J. Chay, *Phys. Lett.* **B476**, 339 (2000); T. Muta et al., *Phys. Rev. D* **62**, 094020 (2000); D. S. Du, D. .S. Yang and G. H. Zhu, *Phys. Lett.* **B488**, 46 (2000); M. Z. Yang and Y. D. Yang, *Phys. Rev. D* **62**, 114019 (2000); J. Chay and C. Kim, hep-ph/0009244; X. -G. He, J. -P. Ma and C. -Y. Wu, *Phys. Rev. D* **63**, 094004 (2001); H. -Y. Cheng and K. -C. Yang, *Phys. Lett.* **B511**, 40 (2001); *Phys. Rev. D* **63**, 074011 (2001); M. Chiuchini et al., hep-ph/0110022; D. K. Ghosh et al., hep-ph/0111106; R. Mohanta, hep-ph/0205297.
- [6] F. Gabbiani et al., *Nucl. Phys.* **B477**, 321 (1996).
- [7] R. Barbieri, A. Strumia, *Nucl. Phys.* **B508**, 3 (1997).
- [8] J. M. Gerard et al., *Phys. Lett.* **B140**, 349 (1984); J. S. Hagelin, S. Kelley, T. Tanaka, *Mod. Phys. Lett.* **A8**, 2737 (1993); T. Goto, T. Nihei and Y. Okada, *Phys. Rev. D* **53**, 5233 (1996); *Erratum-ibid.* **D54**, 5904 (1996); C.-K. Chua and W.-S. Hou, *Phys. Rev. Lett.* **86**, 2728 (2001); hep-ph/0110106; A. Arhrib, C.-K. Chua, and W.-S. Hou, *Eur. Phys. J.* **C21**, 567 (2001); D. Becirevic et al., hep-ph/0112303; D. Chang et al, and R. Sinha, *Phys. Rev. D* **65**, 055010 (2002).
- [9] S. Bertolini, F. Borzumati and A. Masiero, *Phys. Lett.* **B192**, 437 (1987); N. Oshimo, *Nucl. Phys.* **B404**, 20 (1993); S. Bertolini and F. Vissani, *Z. Phys.* **C67**, 513 (1995);

- C.-K. Chua, X.-G. He, W.-S. Hou, *Phys. Rev. D* **60**, 014003 (1999); T. Goto et al., *Phys. Lett.* **B460**, 333 (1999); A. Ali and E. Lunghi, *Eur. Phys. J.* **C21**, 683 (2001); E. Lunghi and D. Wyler, *Phys. Lett.* **B521**, 320 (2001); M.B. Causse and J. Orloff, *Eur. Phys. J.* **C23**, 749 (2002); F. Borzumati et al., *Phys. Rev. D* **62**, 075005 (2000); S. Pokorski, J. Rosiek and C. A. Savoy, *Nucl. Phys.* **B570**, 81 (2000); A.J. Buras et al., *Nucl. Phys.* **B592**, 55 (2001).
- [10] S. Bertolini, F. Borzumati and A. Masiero, *Nucl. Phys.* **B294**, 321 (1987); S. Bertolini et al., *Nucl. Phys.* **B353**, 591 (1991); J.S. Hagelin, S. Kelley, and T. Tanaka, *Nucl. Phys.* **B415**, 293 (1994).
- [11] G. C. Branco et al., *Phys. Lett.* **B337**, 316 (1994); *Nucl. Phys.* **B449**, 483 (1995).
- [12] L. J. Hall, V. A. Kostelecky and S. Raby, *Nucl. Phys.* **B267**, 415 (1986).
- [13] X.-G. He, J.-Y. Lieu and J.-Q. Shi, *Phys. Rev. D* **64**, 094018 (2001).
- [14] V. M. Braun and I. E. Filyanov, *Z. Phys.* **C48**, 239 (1990), P. Ball, *J. High Energy Phys.* **9901**, 010 (1999).
- [15] S. J. Richichi, et al., (CLEO Collaboration), *Phys. Rev. Lett.* **85**, 520(2000); S. Chen, et al., (CLEO Collaboration), *Phys. Rev. Lett.* **85**, 525(2000); A. Bornheim, et al., (CLEO Collaboration), hep-ex/0302026.
- [16] Tomonobu Tomura, (Belle Collaboration), 38th Rencontres de Moriond, ElectroWeak Interactions and Unified Theories, Les Arcs, France, March 15-22, 2003. K.Abe et al., (Belle Collaboration), *Phys. Rev.* **D67**, 031102(2003), [hep-ex/0212062]; Y.Unno, K.Suzuki, et al., (Belle Collaboration), hep-ex/0304035.
- [17] Stephane Willocq, (The BaBar Collaboration), *Nucl. Phys. Proc. Suppl.* **111**, 34(2002); B. Aubert, et al., (The BaBar Collaboration), e-print hep-ex/0206053; B. Aubert, et al., (The BABAR Collaboration), *Phys. Rev. Lett.* **89**281802(2002); B. Aubert, et al., (The BABAR Collaboration), e-print hep-ex/0207065; B. Aubert, et al., (The BABAR

- Collaboration), e-print hep-ex/0303028; B. Aubert, et al., (The BABAR Collaboration), e-print hep-ex/0303039; B. Aubert, et al., (The BABAR Collaboration), e-print hep-ex/0303046.
- [18] Particle Data Group, *Phys. Rev.* **D 66**, 1(2002).
- [19] R. Barate *etal.* (ALEPH Collaboration), *Phys. Lett.* **B429**, 169 (1998), K. Abe *etal.* (Belle Collaboration), *Phys. Lett.* **B511**, 151 (2001); F. Blanc, *talk presented at the XXXVIth Rencontres de Moriond*, Les Arcs, March 2001.
- [20] M. Ciuchini et al., *Phys. Lett.* **B334**, 137 (1994); A. J. Buras et al., *Nucl. Phys.* **B424**, 374 (1994).
- [21] N. Cabbibo and L. Maiani, *Phys. Lett.* **B79**, 109 (1978); M. Suzuki, *Nucl. Phys.* **B145**, 420 (1978); N. Cabbibo, G. Corbe and L. Maiani, *Phys. Lett.* **B155**, 93 (1979).
- [22] A. J. Buras et al., *Nucl. Phys.* **B566**, 3 (2000).
- [23] A. Kagan and M. Neubert, *Eur. Phys. J.* **C7**, 5 (1999); *Phys. Rev. D* **58**, 094012 (1998).
- [24] J. A. Bagger, K. T. Matchev, R. -J. Zhang, *Phys. Lett.* **B412**, 77 (1997).
- [25] A. J. Buras, e-print hep-ph/0101336.
- [26] <http://lepbose.web.cern.ch/LEPBOSC>, 38th Rencontres de Moriond, ElectroWeak Interactions and Unified Theories, Les Arcs, France, March 15-22, 2003.
- [27] B. Aubert, et al., (The BaBar Collaboration), hep-ex/0207073.
- [28] A. Ali and C. Grueb, *Phys. Lett.* **B287**, 191 (1992); A. Ali, V. M. Braun, H. Simma, *Z. Phys.* **C63**, 437 (1994); T. Huang and Z. -H. Li, *Phys. Rev. D* **57**, 1993 (1998); T. Huang, Z. Li, and H. Zhang, *J. Phys.* **G25** 1179 (1999);